Feature-based attentional tuning during biological motion detection measured with SSVEP

Rakibul Hasan
Department of Cognitive Sciences, University of California, Irvine, CA, USA

Ramesh Srinivasan
Department of Cognitive Sciences, University of California, Irvine, CA, USA

Emily D. Grossman
Department of Cognitive Sciences, University of California, Irvine, CA, USA

Performance in detection tasks can be improved by directing attention to task-relevant features. In this study, we evaluate the direction tuning of selective attention to motion features when observers detect point–light biological motion in noise. Feature-based attention strategy is assessed by capitalizing on the sensitivity of unattended steady-state visual-evoked potential (SSVEP) to the spreading of feature-based attention to unattended regions of space. Participants monitored for the presence of a point–light walker embedded in uniform dynamic noise in the center of the screen. We analyzed the phase-locked electroencephalogram response to a flickering random-dot kinematogram (RDK) in an unattended peripheral annulus for the 1 s prior to the onset of the target. We found the highest SSVEP power to originate from electrodes over posterior parietal cortex (PPC), with power modulated by the direction of motion in the unattended annulus. The SSVEP was strongest on trials in which the unattended motion was opposite the facing direction of the walker, consistent with the backstroke of the feet and with the global direction of perceived background motion from a translating walker. Coherence between electrodes over PPC and other brain regions successfully predicted individual participant's d-prime, with the highest regression coefficients at electrodes over ventrolateral prefrontal cortex (VLPFC). The findings are evidence that functional connectivity between frontal and parietal cortex promote perceptual feature-based attention, and subsequent perceptual sensitivity, when segregating point–light figures from masking surround.

Introduction

Feature-based attention is often implicated as the mechanism by which we selectively attend to a limited set of objects in a cluttered environment and effectively ignore, or filter, distracting items from our awareness. Feature-based attention acts upon diagnostic elements in complex scenes to promote detection and recognition, often without explicit knowledge of the observer (i.e., Driver et al., 1999; Gosselyn & Schyns, 2001; New, Cosmides, & Tooby, 2007).

A key example of this is action recognition from point–light animations, in which selective attention binds the unique trajectories of body parts into a perceptually coherent whole (Johansson, 1973; Wittinghofer, de Lussanet, & Lappe, 2012). Although seemingly effortless, integrating the local elements of point–light walkers is attentively demanding. Visual searches for point–light walkers among distractors proceed serially, as would be expected from a feature-based conjunction search (Cavanagh, Labianca, & Thornton, 2001; Mayer, Vuong, & Thornton, 2015), and discriminating point–light actions suffers in dual-task paradigms that make demands on the capacity limited attentional system (Chandrasekaran, Turner, Bulthoff, & Thornton, 2010). Moreover, point–light biological motion sequences constructed from rapidly changing local elements that defeat local motion signals are readily recognized (Beintema & Lappe, 2002; Tyler & Grossman, 2011), while those constructed from complex local elements that discourage binding the local elements are not readily recognized (Wittinghofer, de Lussanet, & Lappe, 2010).

While the importance of attention to the recognition of biological motion is clear from these studies, what

Citation: Hasan, R., Srinivasan, R., & Grossman, E. D. (2017). Feature-based attentional tuning during biological motion detection measured with SSVEP. *Journal of Vision*, *17*(9):22, 1–12, doi:10.1167/17.9.22.

doi: 10.1167/17.9.22 Received January 18, 2017; published August 24, 2017 ISSN 1534-7362

remains uncertain is the nature of the features onto which visual attention is directed. Whereas some computational models argue that biological motion perception proceeds via a skeletal template matching algorithm (Beintema & Lappe, 2002; Thurman & Lu, 2013), most studies implicate characteristic dynamic body movements (Hiris, 2007; Giese & Poggio, 2003; Saunders, Suchan, & Troje, 2009; Thirkettle, Benton, & Scott-Samuel, 2009; Thurman, Giese, & Grossman, 2010; Thurman & Grossman, 2008; Troje, 2002). The two most commonly reported features are the backstroke of the feet (Saunders et al., 2009) and the crossing of joints visible in profile views of locomotion (Giese & Poggio, 2003; Thurman & Grossman, 2008). Neurons tuned to point–light actions typically display selectivity for consistent combinations of body postures and body dynamics (Oram & Perrett, 1996; Vangeneugden, Vancleef, Jaeggli, VanGool, & Vogels, 2010; Vangeneugden et al., 2011).

In addition to features embedded within the actor itself, a body of work exists demonstrating that the visual processes engaged when organizing point–light walkers also influence perception of the surround. Illustrated by the so-called "backscroll illusion," observers experience illusory motion of the background when viewing a stationary point–light walker (lacking translation, as if on a treadmill), with the background perceived to be moving in the opposite direction of the walker (Fujimoto, 2003; Fujimoto & Yagi, 2008). This illusory motion is sufficiently powerful so as to capture and bias the perceived motion of random motion elements in favor of the background when superimposed on point–light sequences (Fujimoto & Yagi, 2007).

In this study, we use a novel neurophysiological approach to isolate the motion features observers selectively attend that promote point–light biological motion detection. In tasks with known targets, selective attention filters are employed in anticipation of the attended items, to bias perceptual encoding in favor of those features (Bridwell, Hecker, Serences, & Srinivasan, 2013; Bridwell & Srinivasan, 2012). Feature-based attention is also not spatially specific, with attention-mediated gain observed in neural populations in visual cortex tuned to the attended feature across visual field (Saenz, Buracas, & Boynton, 2002; Serences & Boynton, 2007). This phenomenon is also predicted from single-unit recordings of feature-based attention gain control, which is not spatially selective (Treue & Martínez Trujillo, 1999). Features and object categories can also be decoded from the neural activity in parietal cortex, an important brain region for cortical control of attention (Erez & Duncan, 2015; Liu & Hou, 2013). This finding is also consistent with early steady-state visual-evoked potential (SSVEP) studies that find parietal responses to be modulated by feature-based attention (Bridwell & Srinivasan, 2012; Bridwell et al., 2013).

We have developed a paradigm to measure these attentionally mediated modulations for attended motion features using probe stimuli in unattended locations that are flickered to evoke a robust SSVEP (Bridwell et al., 2013; Bridwell & Srinivasan, 2012). SSVEP signal modulation is associated with different cognitive and sensory phenomena, and in particular, selective attention (Ding, Sperling, & Srinivasan, 2006; Morgan, Hansen, & Hillyard, 1996; Müller et al., 2006). Important for this study, frequency-tagged SSVEPs can capture the attention modulation of neural signals that share features with the attended objects, *even when the SSVEP is tagged to unattended and spatially displaced stimuli* (Bridwell et al., 2013; Bridwell & Srinivasan, 2012; Garcia, Srinivasan, & Serences, 2013; Painter, Dux, Travis, & Mattingley, 2014).

We therefore seek to use the attentionally-mediated SSVEP as a means for evaluating the directional selectivity of the attentive filters deployed when detecting a biological motion target. Given that subjects use task-relevant knowledge to anticipate diagnostic features, we reason that evidence for features-based attention should be apparent in the brain response throughout the interval during which subjects monitor for appearance of the walker. That includes prior to the actual appearance of the target when the walker is anticipated but not yet perceived. And because neurons tuned to those diagnostic features exhibit attentional gain throughout the visual field, we should be able to identify this attentional strategy in the SSVEP modulations for the flicker-tagged, unattended stimulus when it contains task-relevant features. If observers monitor for local opponent motion when detecting a point–light walker, this should be apparent in brain responses for task-irrelevant motion in both the forward and backward walking directions. If observers monitor for a global body posture, we should not observe any attention modulation on task-irrelevant motion features. Finally, if observers attend to the illusory motion of the background, we should observe attention gain in task-irrelevant motion opposite to that of the facing direction of the walker.

Materials and methods

Participants

The study included 19 unpaid participants (22 to 34 years old, 10 males and nine females) with normal or corrected-to-normal vision. All data was collected in two sessions, and data from three subjects was removed

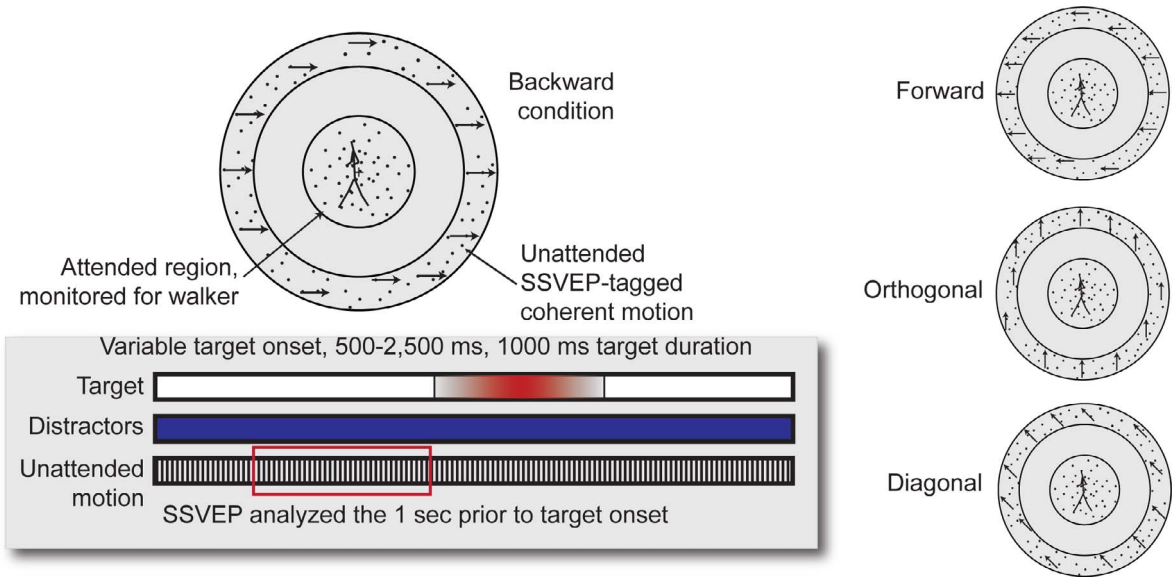

Figure 1. Sample frame of the stimulus (top) and a timeline of the trial events (bottom). The central region of the stimulus contained randomly moving noise dots, a subset of which briefly (500 ms) morphed into a coherent point–light walker. The skeleton figure walker shown in this schematic is for illustrative purposes only and was not visible during the experiment. Subjects monitored this region for the presence of the intact point–light walker, which could appear anywhere from 500–2500 ms following the onset of the trial. The peripheral region of the stimulus was populated with dots moving 100% coherently in one of four possible directions. Backward-directed motion is shown in the main figure, with the other three directions shown in the right panel.

from the analysis because of excessive noise in the electroencephalogram (EEG) data.

Materials

Stimuli

All experimental stimuli were presented in Matlab 2013a (MathWorks, Inc., Natick, MA) using Psychtoolbox 3.0 (Brainard, 1997), and were displayed on an LED monitor set to 60 Hz refresh rate. The visual stimulus was designed with two key regions as shown in Figure 1. The central *attended* region subtended 3.1° visual angle, and a peripheral *unattended* annulus encircled the attended region (6.2°–9.91° visual angle). The two regions were separated by 3.1° and delineated with a black circular line.

The central attended region was populated by small black dots of that moved with a constant velocity in random directions uniformly sampled from all possible orientations (random dot kinematogram, or RDK). Shortly after the onset of the trial, a subset (the "target" dots) transitioned to velocity trajectories were consistent with the 13 major joints and head of a walker at the most salient 500 ms interval of the gait cycle (when the ankles and legs cross; Thurman & Grossman, 2008). In half the trials, the initial starting positions of the dots were carefully constructed such that this transition occurred when those dots had arranged into spatial positions consistent with that of the profile view of a point–light walker (the walker present trials). In the other half of the trials, the initial starting positions of the target dots were constructed such that the transition occurred when the dots were randomly arranged within a virtual box of the approximate same size as the target walker (walker absent "scrambled" trials). At the completion of the gait segment, the target dots smoothly returned to the uniform velocities at which they traveled prior to the target interval. Throughout the trial, the nontarget dots in the central region maintained their constant velocity, serving as a mask by which to increase the difficult level for detecting the coherent walkers. The number of masking noise dots was calibrated for each subject so as to equate detection performance across individuals. All dots, target or masking noise, were displayed as black against a white background and subtended 0.13° visual angle.

The unattended peripheral annulus contained 100 dots dispersed throughout the annulus that moved uniformly and coherently in one of the four possible directions: consistent with the facing direction of the walker ("0°" or "forward"), in the opposite direction as the facing side of the walker ("180°" or "backward"), upward ("90°" or "orthogonal"), or diagonally upward ("45°" or "diagonal"). In addition to the constant velocity, the peripheral annulus dots were frequency tagged using a counterphase flickered (on–

off) at 15 Hz with 50% duty cycle (33 ms on, 33 ms off). Each of the peripheral dots subtends 0.19° visual angle.

Procedure

Participants were instructed to keep their eyes fixated in the central attended region and to monitor for the brief (500 ms) presence of an intact point–light walker, which occurred on half the trials (a detection task). Trials were a total of 3 s in duration, and morphing was initiated at a variable onset between trials (following an exponential decay function) of 500 ms and 2500 ms after the trial start. Half the participants monitored for a leftward facing point–light walker, and the other half monitored for a rightward facing point–light walker. The participants were informed prior to the start of the experiment as to the target facing direction, and were given practice detecting the target on calibration trials (see the following material). Subjects completed 480 trials over the course of eight blocks (60 trials each).

Psychophysical calibration

Before completing the main experiment, each subject participated in a calibration session in which we estimated the number of masking distractor dots in the central region required to obtain equivalent performance across individuals. Calibration proceeded as a 2–1 double interleaved staircase design in which the number of distractor dots increased following two successive correct trials, and decreased following a single incorrect trial. Subjects were not given feedback on their performance after each trial. This procedure, completed for two independent and interleaved staircases, converged on the number of noise dots that yields 71% accuracy in the detection task. The total number of trials was 150 and the number of required distractor dots determined using mean of the last five reversals of each of the staircases. Trials in the main experiment were identical to the calibration, with the exception that the number of dots masking the target figure was fixed at the individually calibrated level.

Behavioral data from the main experiment was analyzed using signal detection theory in which d-prime, a perceptual sensitivity index, is computed independently from decision criteria. Subject responses were categorized as hits, misses, correct rejections, or false alarms, and d-prime was computed using cumulative normal distribution corresponding to the hit rate and false-alarm rate.

$$Dprime = Z(HitRate) - Z(FalseAlarmRate) \quad (1)$$

EEG acquisition and analysis

EEG measurements were collected during the main experiment using a 128 channel Hydrocel Geodesic Sensor Net (Electrical Geodesics, Eugene, OR) equipped with a photocell system to give accurate and fast sampling of each cycle of the peripheral flickering stimulus. The EEG signals were recorded with a 1000 Hz sampling rate and low-pass filtered at 50 Hz.

We analyzed data from correct trials from the four unattended motion direction conditions (forward, backward, orthogonal, and diagonal) using the 1000 ms of phase-locked EEG signal prior to target onset. We removed nuisance noise (e.g., eye blink and muscle movements) using Infomax independent component analysis (Bell & Sejnowski, 1995) and then applied a fast Fourier transform (Matlab; MathWorks) to perform Fourier transform on the time series data to convert into frequency domain. Then, for each condition c at each electrode e we calculated SSVEP power by averaging the Fourier coefficients F_n at the flicker frequency f over N trials as

$$Power_{e,c} = \left| \frac{1}{N} \sum_{n=1}^{N} F_n \right|^2 \quad (2)$$

Here, F_n refers to Fourier coefficient on trial n; e refers to electrode, and N refers to total number of trials. Then, we calculated mean SSVEP power over all the conditions at each electrode for SSVEP frequency as

$$M_e(f) = \frac{1}{4} \sum_{c=1}^{4} Power_{e,c}(f) \quad (3)$$

To eliminate electrodes with insufficient SSVEP power, we computed a signal-to-noise ratio for the mean SSVEP power at each electrode (M_e) as the ratio of the power at the SSVEP frequency of 15 Hz (with a 1Hz bandwidth) to the average of each of the four surrounding center frequencies (13, 14, 16, 17 Hz). These four frequencies were selected to obtain an estimate of the background power at 15 Hz as they symmetrically surround the stimulus frequency and all fall within the beta band. Signal-to-noise ratios were used to select the channels with robust SSVEP responses.

The mean normalized SSVEP was used as a metric for attentional tuning. At each electrode, we calculated normalized SSVEP power for each condition as the fractional modulation with respect to the average SSVEP power over all the conditions.

$$MeanNormalizedPower_{e,c} = \frac{Power_{e,c}(f) - M_e(f)}{M_e(f)} \quad (4)$$

Coherence and partial least squares (PLS) regression

EEG coherence is used as an estimate of functional connectivity (Srinivasan, Bibi, & Nunez, 2006; Winter, Nunez, Ding, & Srinivasan, 2007). Coherence is the squared correlation coefficient that estimates the consistency of relative amplitude and phase between any two pair of electrodes/sources at each frequency band (Bendat & Piersol, 2000). For a given frequency, a coherence value of 1 indicates signals with exactly the same phase difference and amplitude ratio on each trial, while coherence approaches 0 if the signals have a random difference in phase and amplitude ratio. In practice, EEG coherence depends mostly on the consistency of phase differences between electrodes (Srinivasan et al., 2006). For our data, we were interested to look at strength of phase-locking across the brain with respect to a particular seed region, and therefore calculated coherence matrix across electrodes at the SSVEP frequency.

Coherence was then used as an independent variable for predicting individual subject perceptual sensitivity using partial least squares (PLS). The PLS models were computed using the N-way toolbox (Andersson & Bro, 2000). Data were first mean-centered, then subjected to direct orthogonal signal correction (DOSC) to remove the largest component of the predicting data (SSVEP coherence or power) that was orthogonal to the behavioral data (d-prime) before applying PLS to allow for more efficient PLS models with fewer components (Krishnan, Kang, Sperling, & Srinivasan, 2013; Svensson, Kourti, & MacGregor, 2002).

We generated a new PLS model for each condition of motion direction (in the unattended peripheral annulus). We determined the predictive values for each of the four PLS models using a leave-one-out cross-validation procedure in which data from one participant was iteratively removed from the PLS model and the remainder of the subjects' data were used as a training set. As used in previous studies using PLS, we considered as many components as needed to explain at least 80% of fitted behavioral variance to retain in the model (Krishnan et al., 2013; Wu, Srinivasan, Kaur, & Cramer, 2014). Models with either less or more components did not perform as well in the cross-validation. We then tested the extent to which the trained model could predict the d-prime sensitivity of the one excluded subject, and repeated this process for each subject. Model performance was estimated using the difference between predicted and actual d-prime for each subject, we calculated the predicted R^2 for each condition.

Results

Behavior

Subjects detected the presence of point–light walkers within the dynamic mask with mean accuracy of 80.0%, which was expected because task difficulty was calibrated prior to the onset of the main experiment. This corresponded to an average d-prime sensitivity score of 2.31 (*SD*: 0.81), and an average criterion score of 0.33 (*SD*: 0.52). A one-way repeated-measures analysis of variance (ANOVA) showed no significant effect of the direction of motion in the unattended peripheral annulus on sensitivity or criterion, ($F(3, 60) = 0.15$, $p = 0.92$; $F(3, 60) = 0.08$, $p = 0.97$, respectively).

SSVEP

Our SSVEP analysis targeted those electrodes with the highest signal-to-noise (SNR) ratio estimates, which corresponded with electrodes overlying three brain regions: posterior parietal cortex (PPC), left occipital cortex, and right occipital cortex (Figure 2A). A one-way repeated-measures ANOVA revealed significant differences in the SSVEP power of the electrodes over PPC depending on the direction of unattended motion in the unattended peripheral annulus, $F(3, 60) = 9.97$, $p < 0.001$. A post-hoc t test indicated significantly higher power over the PPC for those trials in which the unattended motion moved opposite to the facing direction of the walker (backward condition, Figure 2B), as compared with the forward, diagonal, or orthogonal conditions ($p = 0.002$, $p < 0.001$, and $p = 0.007$, respectively). In contrast, we found no significant influence of unattended motion on the SSVEP power over right occipital cortex (Figure 2D), $F(3, 60) = 1.46$, $p = 0.23$, and a marginal effect of motion direction over left occipital cortex (Figure 2C), $F(3, 60) = 2.44$, $p = 0.07$.

PLS regression

From the findings discussed so far we conclude the SSVEP in posterior parietal cortex has information as to the attentional filter applied by the observers, when monitoring for the onset of the target but prior to perceptual encoding. We therefore sought to determine whether there exists a relationship between the neural

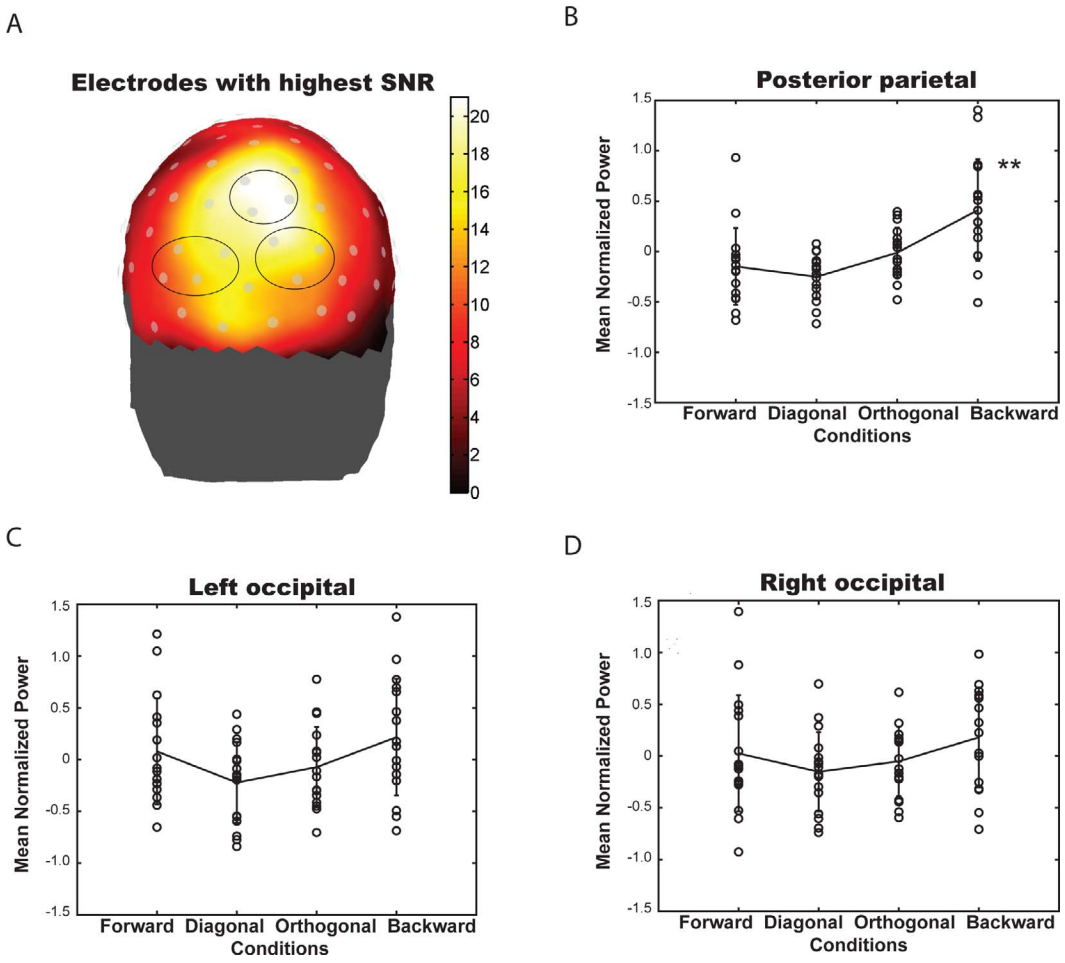

Figure 2. (A) Topographic map of the average signal-to-noise ratio (SNR) of the SSVEP during the anticipatory interval, across all conditions. Electrodes over posterior parietal regions had the highest SSVEP SNR across participants. (B, C, D) Tuning curves of mean normalized SSVEP power for the posterior parietal (three electrodes), left and right occipital region (four and three electrodes, respectively). Forward, diagonal, orthogonal, and backward are with respect to the facing direction of the walker and indicate the direction of peripheral motion. Each circle indicates the mean SSVEP normalized power for each condition (specified by the direction of the unattended motion), for each participant. The solid line indicates the average "tuning curve" across participants.

signals associated with directing attention to backwards motion and individual subject performance. We hypothesized that the extent to which subjects effectively engaged a tuned attentional filter should predict individual subject behavioral performance.

To evaluate the relationship between the SSVEP signals across the subjects and individual subject performance (specifically, d-prime sensitivity) in detecting an upcoming target, we applied a PLS regression method to predict behavioral data from the SSVEP data (Wold, Svante, Ruhe, Wold, & Dunn, 1984). In a previous study, PLS methods successfully predicted acquisition of motor skill in a future task from brain connectivity during resting state (Wu et al., 2014). PLS methods have also been used to identify patterns of neural activation related to changes in task content (McIntosh & Lobaugh, 2004), and has been found useful for defining relationships between measures of brain function and performance in spatial attention tasks (Krishnan, Williams, McIntosh, & Abdi, 2011).

To test our hypothesis, we applied PLS modeling to predict individual subjects' sensitivity (d-prime) from SSVEP power using electrodes located over PPC, and right and left occipital cortex, computed for each condition's data separately. None of these groups of electrodes tested had SSVEP power, for any condition, that could successfully predict d-prime values from SSVEP ($R^2 < 0.01$ for all the conditions). Additionally, we repeated this analysis for all the electrodes (excluding those with artifacts) as independent variables instead of taking regional electrodes only, but found no evidence that SSVEP power predicts d-prime sensitivity.

We did, however, find evidence that cortico-cortical connectivity (as reflected in coherence) predicts behav-

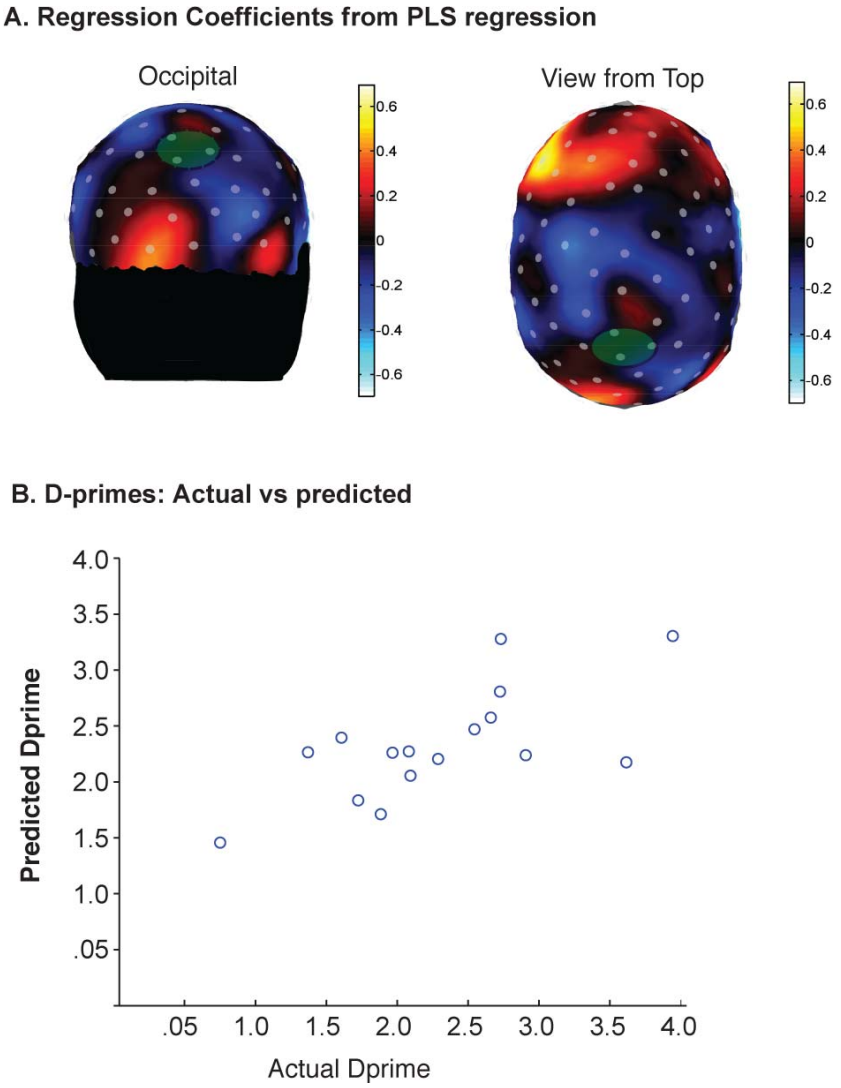

Figure 3. (A) Topographic map of regression coefficients (left: posterior view; right: top view) from the PLS model fitting in which independent variables were coherence estimation of SSVEP at each electrode with respect to the PPC, constructed using the "backward" condition data. Dependent variables are mean d-prime values across the conditions for each subject. (B) Scatterplot of actual d-prime and predicted d-prime from PLS model using backward condition data. Circles indicate participants.

ioral sensitivity. Using PLS cross-validation, we found that coherence between the electrodes of PPC region and all other electrodes successfully predicted individual subject d-prime (sensitivity index) in the backward unattended motion condition (predicted $R^2 = 0.46$). The highest regression coefficients, those electrodes that contributed most strongly to the individual subject's d-prime variance, were located over left ventrolateral prefrontal cortex (VLPFC; Figure 3A), evidence for a frontal–parietal network supporting successful target detection. Positive linear relation between actual and predicted d-prime values from backward unattended motion condition data (Figure 3B) supports successful prediction of individual participant's d-prime from backward condition data using PLS model. No other condition data (forward, diagonal, and orthogonal) could successfully predict d-prime values from connectivity strength between posterior parietal and other brain regions.

We found no feature in the SSVEP coherence scores to successfully predict criterion values from the individual subjects. SSVEP coherence during the monitoring phase only carries information about subject's subsequent perceptual sensitivity, not about criterion shifts in response.

Discussion

In our study, we sought evidence for feature-tuning in the brain while monitoring for the appearance of a

point–light walker embedded in a cluttered array. We found posterior parietal cortex to be modulated by the direction of unattended motion in the periphery, indicative of feature-based attention that is dispersed throughout the visual field. This finding was anticipated based on previous studies capitalizing on the spatially distributed boost in cortical gain for neurons with receptive field tuning matched to the attended features (Martinez-Trujillo & Treue, 2004; Saenz et al., 2002; Serences & Boynton, 2007; Treue & Martinez-Trujillo, 1999).

SSVEP power was significantly higher only when the unattended RDK was moving opposite to the heading direction of the target point-light walker. Because the power was asymmetric, higher for opposite versus the forward facing direction of the walker, we conclude that subjects were not monitoring for local opponent motion (which contains both directional features). Instead, the unattended motion condition with highest SSVEP power most closely matches both that of the backstroke of feet and the perceived illusory movement of the background during gait (the "backscroll illusion"). Both of these features have been previously identified in studies of point–light biological motion encoding as beneficial for promoting point–light target detection in masking arrays (Fujimoto & Sato, 2006; Saunders et al., 2009).

We observe the increased SSVEP power for unattended backward motion prior to observing the action, evidence that subjects are engaging attentional filters while monitoring for the target, the onset of which was uncertain within the extended trial sequence. Moreover, the extent to which subjects engaged those filters predicted sensitivity to target detection. Thus subjects actively engage feature-based attention mechanisms prior to the onset of targets to maximize detection.

Our task involves monitoring for a target that is constructed by diagnostic features that must be segregated from surrounding noise. To achieve this, subjects must employ a guided visual search to enhance task-relevant features and suppress unwanted noise. Previous studies show that synchronization strength between fronto-parietal network and visual cortex carry information regarding target relevant features (Gregoriou, Gotts, Zhou, & Desimone, 2009). From our results, we not only found evidence for attentional modulation in parietal cortex for task-relevant features, but also found behaviorally relevant information in the phase synchronization of a fronto-parietal network tagged by a SSVEP outside of the attentional focus.

The strength of the SSVEP phase-locking coherence between posterior parietal cortex and lateral prefrontal cortex carries information regarding participants' subsequent perceptual sensitivity (d-prime), with predictive information highest when the RDK matches a relevant feature for perceptual encoding. This is not without precedent. In a previous single-unit study, neurons in V4 are modulated by changes in perceptual sensitivity, without any change in criterion shifts (Luo & Maunsell, 2015). Together, this is evidence that there are separate brain networks and/or regions associated with processing of perceptual sensitivity toward the stimuli only. On the other hand, although the fronto-parietal network could predict behavioral performance (e.g., d-prime), individual brain regions alone could not predict information about behavioral performance, which reflects that behavioral performance is linked to coordinated activations of more than one brain region, not to local activations of a particular brain region.

In a previous study using the same paradigm of tagging unattended region with SSVEP, enhancement of task-relevant features was found when using upper alpha range (12 Hz) flickering stimuli (Bridwell et al., 2012). Unlike our findings, that study also revealed evidence of suppression for task-irrelevant features. There could be two possible reasons for the differences between these studies. One reason is that in the previous work, authors found task-relevant suppression in lower alpha range (8 Hz), whereas our study only used one frequency (15 Hz) at beta range. Also, the previous work found suppression in the unattended region when the attended and unattended region had similar background noise flickering at 8 Hz, a design feature that may have made the subjects to engage in attention strategies that included suppressing the background flickering stimuli. In our study, noise at the attended region (coherent motion in all directions) had limited similarity to the unattended features (unidirectional motion, minimizing the need to actively suppress features in the peripheral SSVEP-tagged field. Note that if suppression of irrelevant features contributed to perceptual sensitivity, the PLS model would have been able to predict sensitivity in the forward, diagonal, and orthogonal directions, albeit with regression coefficients of the opposite sign. It was our observation, however, that the SSVEP coherence for irrelevant motion directions did not predict sensitivity. Our results are consistent with another study using the same SSVEP paradigm where feature-based enhancement of unattended SSVEP was found when subjects had to perform an attentionally demanding task (during visual conjunction search, not during unique feature task; Painter et al., 2014) and no suppression was observed.

In this study, we found attentional enhancement for unattended motion that moved opposite the facing direction of the walker, consistent with one local and one global feature. The local feature, the backstroke of the feet, is a salient cue for walker detection present in natural point–light motion but often missing in simulated locomotion (Saunders et al., 2009). The illusory motion of the background is a global feature associated with perceptual organization of dynamic

objects (but not disconnected object features; Fujimoto, 2003; Fujimoto & Sato, 2006; Fujimoto & Yagi, 2008). Individuals experience this illusory motion when detecting an intact point–light walker, but not with scrambled walkers (Fujimoto & Sato, 2006; Fujimoto & Yagi, 2007), and when point–light walkers are embedded in dynamic noise the illusory motion of the background captures and strengthens the perceived motion energy of masking noise elements (Fujimoto & Sato, 2007). Thus the perceived motion of the background is a potent cue for driving attentional modulation of the SSVEP-tagged unattended surround and could facilitate detection of the masked point–light figure.

Additionally, the tuning of the attentional modulation we observed was much stronger in PPC than in early visual cortex. A comparison between the tuning curves between the electrodes over these two regions indicates stronger attention bias consistent with backward motion in the PPC, with smaller attentional bias in early visual cortex during both the forward and backward conditions. This suggests that parietal cortex is more reflective of feature-based attention tuning than early visual areas.

An alternative explanation arises from the possibility of motion adaptation for biological motion. In a previous study, individuals experienced motion adaptation for the global heading direction of point–light biological motion when exposed for a long period of time (90 s), with no evidence for adaptation when viewing local dot motion (Jackson & Blake, 2010). In our experiment, however, we note that unambiguous point–light walkers were only present for 500 ms on half the trials, with incoherent translating motion present for the remaining 2.5 s. Considering that our findings are based on data from portion of trial that contained only scrambled bio-motion and masking dots, and we feel the increase in SSVEP power for unattended feature is unlikely to have arisen from motion adaptation; rather, it is more likely to be an effect of attentional monitoring.

Conclusion

Our study identifies neural tuning to relevant features for human walker detection using a point–light human walker embedded in a noisy background. Evidence shows the observers monitor for motion opposite the facing direction of the walker, and this feature matches with the backstroke of the feet and the direction of "backscroll illusion" while detecting a human walker. Our study also finds that brain connectivity strength of fronto-parietal network during monitoring phase of attention can be predictive about subsequent perceptual sensitivity (d-prime) in healthy human participants. This indicates that behavioral performance in our task was dependent on the state of communication between posterior parietal and lateral prefrontal brain regions during the monitoring phase of the task. Additionally, as identified fronto-parietal network could predict only perceptual sensitivity, not decision criteria, that particular fronto-parietal network during monitoring phase was most likely involved in processing subjective quality of signal associated with task only, not internal response bias of participants.

In our study, we tagged only peripheral unattended region and analyzed data before the target onset to exclude any influence of decision criteria on the measurement of attentional feature selectivity. To identify brain networks associated with change in decision criteria, in a future study, we can tag the target region with a distinct frequency in beta range and analyze the data after target onset.

Keywords: biological motion, EEG, feature-based attention, SSVEP

Acknowledgments

Commercial relationships: none.
Corresponding author: Emily D. Grossman.
Email: grossman@uci.edu.
Address: Department of Cognitive Sciences, University of California—Irvine, Irvine, CA, USA.

References

Andersson, C. A., & Bro, R. (2000). The N-way Toolbox for MATLAB. *Chemometrics and Intelligent Laboratory Systems*, *52*, 1–4. https://doi.org/10.1016/S0169-7439(00)00071-X

Beintema, J. A., & Lappe, M. (2002). Perception of biological motion without local image motion. *Proceedings of the National Academy of Sciences, USA*, *99*(8), 5661–5663. http://doi.org/10.1073/pnas.082483699

Bell, A. J., & Sejnowski, T. J. (1995). An information-maximization approach to blind separation and blind deconvolution. *Neural Computation*, *7*(6), 1129–1159.

Bendat, J. S., & Piersol, A. G. (2000.) *Random data: analysis and measurement procedures, 3rd edition.* New York: Wiley.

Brainard, D. H. (1997). The Psychophysics Toolbox. *Spatial Vision*, *10*, 433–436.

Bridwell, D. A., Hecker, E. A., Serences, J. T., & Srinivasan, R. (2013). Individual differences in attention strategies during detection, fine discrimination, and coarse discrimination. *Journal of Neurophysiology*, *110*(3), 784–794. http://doi.org/10.1152/jn.00520.2012

Bridwell, D., & Srinivasan, R. (2012). Distinct attention networks for feature enhancement and suppression in vision. *Psychological Science*, *23*(10), 1151–1158. http://doi.org/10.1177/0956797612440099

Cavanagh, P., Labianca, A. T., & Thornton, I. M. (2001). Attention-based visual routines: Sprites. *Cognition*, *80*(1-2), 47–60. http://doi.org/10.1016/S0010-0277(00)00153-0

Chandrasekaran, C., Turner, L., Bulthoff, H. H., & Thornton, I. M. (2010). Attentional networks and biological motion. *Psihologija*, *43*(1), 5–20. http://doi.org/10.2298/PSI1001005C

Ding, J., Sperling, G., & Srinivasan, R. (2006). Attentional modulation of SSVEP power depends on the network tagged by the flicker frequency. *Cerebral Cortex*, *16*(7), 1016–1029. http://doi.org/10.1093/cercor/bhj044

DriverIV, J., G., Davis, P., Ricciardelli, P., Kidd, E., Maxwell, & S. Baron-Cohen, (1999). Gaze perception triggers reflexive visuospatial orienting. *Visual Cognition*, *6*(5), 509–540.

Erez, Y. & Duncan, J. (2015). Discrimination of visual categories based on behavioral relevance in widespread regions of frontoparietal cortex. *Journal of Neuroscience*, *35*(36), 12383–12393.

Fujimoto, K. (2003). Motion induction from biological motion. *Perception*, *32*(10), 1273–1277.

Fujimoto, K., & Sato, T. (2006). Backscroll illusion: Apparent motion in the background of locomotive objects. *Vision Research*, *46*(1), 14–25.

Fujimoto, K., & Yagi, A. (2007). Backscroll illusion in far peripheral vision. *Journal of Vision*, *7*(8):16, 1–7, doi:10.1167/7.8.16. [PubMed] [Article]

Fujimoto, K., & Yagi, A. (2008). Biological motion alters coherent motion perception. *Perception*, *37*(12), 1783–1789.

Garcia, J. O., Srinivasan, R., & Serences, J. T. (2013). Near-real-time feature-selective modulations in human cortex. *Current Biology: CB*, *23*(6), 515–522. http://doi.org/10.1016/j.cub.2013.02.013

Giese, M. A., & Poggio, T. (2003). Neural mechanisms for the recognition of biological movements. *Nature Reviews Neuroscience*, *4*(3), 179–192.

Gosselin, F., & Schyns, P. G. (2001). Bubbles: A technique to reveal the use of information in recognition tasks. *Vision Research*, *41*(17), 2261–2271.

Gregoriou, G. G., Gotts, S. J., Zhou, H., & Desimone, R. (2009, May 29). High-frequency, long-range coupling between prefrontal and visual cortex during attention. *Science*, *324*(5931), 1207–1210. http://doi.org/10.1126/science.1171402

Hiris, E. (2007) Detection of biological and nonbiological motion. *Journal of Vision*, *7*(12):4, 1–16, doi: 10.1167/7.12.4. [PubMed] [Article]

Jackson, S., & Blake, R. (2010). Neural integration of information specifying human structure from form, motion, and depth. *The Journal of Neuroscience*, *30*(3), 838. http://doi.org/10.1523/JNEUROSCI.3116-09.2010

Johansson, G. (1973). Biological Motion, *14*(2), 1–2. http://doi.org/10.3758/BF03212378

Krishnan, A., Williams, L. J., McIntosh, A. R., & Abdi, H. (2011). Partial Least Squares (PLS) methods for neuroimaging: A tutorial and review. *Neuroimage*, *56*(2), 455–475.

Krishnan, L., Kang, A., Sperling, G., & Srinivasan, R. (2013). Neural strategies for selective attention distinguish fast-action video game players. *Brain Topography*, *26*(1), 83–97.

Liu, T. & Hou, Y. (2013). A hierarchy of attention priority signals in human frontoparietal cortex. *Journal of Neuroscience*, *33*(42), 16606–16616.

Luo, T., & Maunsell, J. (2015). Neuronal modulations in visual cortex are associated with only one of multiple components of attention. *Neuron*, *86*(5), 1182–1188.

Martinez-Trujillo, J. C., & Treue, S. (2004). Feature-based attention increases the selectivity of population responses in primate visual cortex. *Current Biology*, *14*(9), 744–751. http://doi.org/10.1016/j.cub.2004.04.028

Mayer, K. M., Vuong, Q. C., & Thornton, I. M. (2015). Do people "pop out"? *PLoS ONE*, *10*(10), 1–15. http://doi.org/10.1371/journal.pone.0139618

McIntosh, A. R., & Lobaugh, N. J. (2004). Partial least squares analysis of neuroimaging data: Applications and advances. *Neuroimage*, *23*, S250–S263.

Morgan, S. T., Hansen, J. C., & Hillyard, S. A. (1996). Selective attention to stimulus location modulates the steady-state visual evoked potential. *Proceedings of the National Academy of Sciences, USA*, *93*(10), 4770–4774. http://doi.org/10.1073/pnas.93.10.4770

Müller, M. M., Andersen, S., Trujillo, N. J., Valdés-Sosa, P., Malinowski, P., & Hillyard, S. A. (2006).

Feature-selective attention enhances color signals in early visual areas of the human brain. *Proceedings of the National Academy of Sciences, USA*, *103*(38), 14250–14254. http://doi.org/10.1073/pnas.0606668103

New, J., Cosmides, L., & Tooby, J. (2007). Category-specific attention for animals reflects ancestral priorities, not expertise. *Proceedings of the National Academy of Sciences, USA*, *104*(42), 16598–16603.

Oram, M. W., & Perrett, D. I. (1996) Integration of form and motion in the anterior superior temporal polysensory area (STPa) of the macaque monkey. *Journal of Neurophysiology*, *76*(1), 109–129.

Painter, D. R., Dux, P. E., Travis, S. L., & Mattingley, J. B. (2014). Neural responses to target features outside a search array are enhanced during conjunction but not unique-feature search. *The Journal of Neuroscience*, *34*(9), 3390–3401. http://doi.org/10.1523/JNEUROSCI.3630-13.2014

Saenz, M., Buracas, G. T., & Boynton, G. M. (2002). Global effects of feature-based attention in human visual cortex. *Nature Neuroscience*, *5*, 631–632.

Saunders, D. R., Suchan, J., & Troje, N. F. (2009). Off on the wrong foot: Local features in biological motion. *Perception*, *38*, 522–533. http://doi.org/10.1068/p6140

Serences, J. T., Boynton, G. M. (2007). Feature-based attentional modulations in the absence of direct visual stimulation. *Neuron*, *55*(2), 301–312.

Serences, J. T., Shomstein, S., Leber, A. B., Golay, X., Egeth, H. E., & Yantis, S. (2005). Coordination of voluntary and stimulus-driven attentional control in human cortex. *Psychological Science*, *16*(2), 114–122. http://doi.org/10.1111/j.0956-7976.2005.00791

Srinivasan, R., Bibi, F. A., & Nunez, P. L. (2006). Steady-state visual evoked potentials: Distributed local sources and wave-like dynamics are sensitive to flicker frequency. *Brain Topography*, *18*(3), 167–187. http://doi.org/10.1007/s10548-006-0267-4

Svensson, O., Kourti, T., & MacGregor, J. F. (2002). An investigation of orthogonal signal correction algorithms and their characteristics. *Journal of Chemometrics*, *16*(4), 176–188.

Thirkettle, M., Benton, C. P., & Scott-Samuel, N. E. (2009). Contributions of form, motion and task to biological motion perception. *Journal of Vision*, *9*(3):28, 1–11, doi:10.1167/9.3.28. [PubMed] [Article]

Thurman, S. M., Giese, M. A., & Grossman, E. D. (2010). Perceptual and computational analysis of critical features for biological motion. *Journal of Vision*, *10*(12):15, 1–14, doi:10.1167/10.12.15. [PubMed] [Article]

Thurman, S. M., & Grossman, E. D. (2008). Temporal "Bubbles" reveal key features for point-light biological motion perception. *Journal of Vision*, *8*(3):28, 1–11, doi:10.1167/8.3.28. [PubMed] [Article]

Thurman, S. M., & Lu, H. (2013). Physical and biological constraints govern perceived animacy of scrambled human forms. *Psychological Science*, *24*(7), 1133–1141, doi:10.1177/0956797612467212

Treue, S., & Martínez Trujillo, J. C. (1999). Feature-based attention influences motion processing gain in macaque visual cortex. *Nature*, *399*(6736), 575–579. http://doi.org/10.1038/21176

Troje, N. F. (2002) Decomposing biological motion: A framework for analysis and synthesis of human gait patterns. *Journal of Vision*, *2*(5):2, 371–387, doi:10.1167/2.5.2. [PubMed] [Article]

Tyler, S. C., & Grossman, E. D. (2011). Feature-based attention promotes biological motion recognition. *Journal of Vision*, *11*(10):11, doi:10.1167/11.10.11. [PubMed] [Article]

Vangeneugden, J., De Maziere, P.A., Van Hulle, M.M., Jaeggli, T., Van Gool, L., & Vogels, R. (2011). Distinct mechanisms for coding of visual actions in macaque temporal cortex. *Journal of Neuroscience*, *31*(2), 385–401.

Vangeneugden, J., Vancleef, K., Jaeggli, T., VanGool, L., & Vogels, R. (2010) Discrimination of locomotion direction in impoverished displays of walkers by macaque monkeys. *Journal of Vision*, *10*(4):22, 1–19, doi:10.1167/10.4.22. [PubMed] [Article]

Winter, W. R., Nunez, P. L., Ding, J., & Srinivasan, R. (2007). Comparison of the effect of volume conduction on EEG coherence with the effect of field spread on MEG coherence. *Statistics in Medicine*, *26*(21), 3946–3957. http://doi.org/10.1002/sim.2978

Wittinghofer, K., de Lussanet, M. H., & Lappe, M. (2010). Category-specific interference of object recognition with biological motion perception. *Journal of Vision*, *10*(13):16, 1–11, doi:10.1167/10.13.16. [PubMed] [Article]

Wittinghofer, K., de Lussanet, M. H., & Lappe, M. (2012). Local-to-global form interference in biological motion perception. *Attention, Perception, & Psychophysics*, *74*(4), 730–738.

Wold , Svante , Ruhe, A., Wold, H. & Dunn, W. J.

(1984). The Collinearity Problem in linear regression. The Partial least squares (PLS) approach to generalized inverses. *SIAM Journal on Scientific and Statistical Computing*, *5*(3), 735–743.

Wu, J., Srinivasan, R., Kaur, A., & Cramer, S. (2014). Resting-state cortical connectivity predicts motor skill acquisition, *Neuroimage*, *91*, 84–90. http://doi.org/10.1016/j.neuroimage.2014.01.026